J. Water Environ. Nanotechnol., 5(4): 342-357 Autumn 2020

ORIGINAL RESEARCH PAPER

Effect of Magnetite Nanoparticles Addition on Modification of Cobalamins Production via Propionibacterium *freudenreichii* PTCC1674 Using Oily Sludge of Lubricant Industry as a Carbon Source

Rouhollah Hedayati[1], Morteza Hosseini[1,*], Ghasem D. Najafpour[1], Hosein Attar[2]

[1] *Biotechnology Research Laboratory, Faculty of Chemical Engineering, Babol Noshirvani University of Technology, Babol, Iran.*
[2] *Chemical Engineering Department, Chemical Engineering and Petroleum Faculty, Tehran Science and Research Branch, Islamic Azad University, Tehran, Iran.*

Received: 2020-8-13 Accepted: 2020-10-21 Published: 2020-11-15

ABSTRACT

Cobalamins are one of the most complicated cofactors produced by microorganisms. *Propionibacterium freudenreichii* has to follow the anaerobic and aerobic conditions respectively during a course of batch fermentation, for the production of the biologically active form of cobalamins. Magnetite (Fe_3O_4) nanoparticles can modify gas-liquid volumetric mass transfer coefficient in the fermentation system in order to create a more efficient aeration step. Initially, the modified production of Fe_3O_4 nanoparticles through the coprecipitation method was investigated, and the smallest size of nanoparticles was optimized to 13.86 nm via the Box-Behnken design of response to surface methodology (RSM). The optimum condition was present at the synthesis, including the temperature of 60 °C, reaction duration of 10 minutes, and the medium agitation speed of 700 rpm. Synthesized nanoparticles were characterized by SEM images, PXRD, and EDS analysis; additionally, the EDS spectrum reflects 39.33% of Fe and 51.8% of oxygen atomic distribution, which confirms the Fe_3O_4 nanoparticles synthesis. Magnetite nanoparticle suspension was added to the fermentation medium in order to compare the effects of nanoparticle incorporation and dimethylbenzimidazole addition on the cobalamin production via *Propionibacterium freudenreichii*. NPs incorporation in the fermentation broth was able to increase the cyanocobalamin production by 20%, while there was no incorporation of external DMBI in the medium. Finally, by the central composite design analysis, cyanocobalamin production from *Propionibacterium freudenreichii* fermentation was optimized to 1.548 $mg.L^{-1}$. Oily sludge (as a new carbon source) of 4 %w/v, magnetite nanoparticles suspension of 7.5 %v/v, and the fermentation temperature of 37 °C caused the CCD optimum condition.

Keywords: *Cobalamins biosynthesis; Magnetite Nanoparticles; RSM Optimization; Propionibacterium freudenreichii*

How to cite this article
Hedayati R., Hosseini M., D. Najafpour GH., Attar H. Effect of Magnetite Nanoparticles Addition on Modification of Cobalamins Production via Propionibacterium freudenreichii PTCC1674 Using Oily Sludge of Lubricant Industry as a Carbon Source. J. Water Environ. Nanotechnol., 2020; 5(4): 342-357.
DOI: 10.22090/jwent.2020.04.005

INTRODUCTION

Cobalamins are the most complex organometallic compounds, which are produced via microorganisms (bacteria and alga) [1]. Cyanocobalamin (Cyano-Cbl), the cyanide form of the natural cobalamins, has been categorized as the most stable form of cobalamins in the extracellular environment [2]. The leading role of the intracellular cobalamins is the cofactor

* Corresponding Author Email: *m.hosseini@nit.ac.ir*

consequence. Methylcobalamin (MeCbl) and adenosylcobalamin (AdoCbl) have been addressed as the most studied cobalamin cofactors [3]. AdoCbl initially was discovered as a part of glutamate mutase, and later on, MeCbl was defined as a part of methionine synthase, and both cofactors were reported as highly photosensitive as cobalamin analogues [4]. Besides the Co-C bond at the center of the cobalamin molecules, the upper and lower ligands induce a range of properties to the targeted enzymes [5]. Adenine and dimethylbenzimidazole (DMBI) are known for lower ligands of cobalamin molecules. DMBI carrying cobalamins are biologically active forms [6, 7]. The aerobic and anaerobic pathways for cobalamin production have been well studied [8]. Cobalt chelation is the main difference between the mentioned pathways. Cobalt insertion via an anaerobic pathway in the bacteria like *propionibacterium freudenreichii* appears earlier in comparison with what happens in the *Pseudomonas denitrificans* through *an* aerobic pathway [9, 10].

Propionibacterium freudenreichii (P. freudenreichii) has defined been as gram-positive, anaerobic aerotolerant actinobacteria. The propionic acid, acetic acid, and vitamin B12 have been achieved by *P. freudenreichii* fermentation [11, 12]. This strain carries anomalous metabolic pathways less finding in other bacteria. The *Propionibacterium* genus for propionic acid production is entitled the wood-werkman cycle (w.w.c) [13]. Co-enzyme A (CoA) derivatives and carbon dioxide are synthesized via w.w.c as well [14]. Reversible transcarboxylase reactions in w.w.c involved methyl malonyl-CoA mutase, and it is one of the specific original B12-coenzyme dependent reactions of the diary *Propionibacterium* [15]. In addition to Swiss cheese ripening, eyehole making, and flavoring in the dairy preparation [16], anaerobic vitamin B12 production using *P. freudenreichii* was extremely studied. De novo synthesis of natural cobalamins in *P. freudenreichii* is initiated from aminolevulinic acid synthesis and afterwards crosses porin and porphobilinogen pathway and eventually by DMBI linkage to the adenosylcobinamid-GDP backbone, adoCbl is produced [17, 18]. For a while, it was not clear how DMBI is presented in this species until understanding the role of COT2/BLUB fused gene. BLUB gene codes 5, 6 dimethylbenzimidazole synthases, and via this enzyme, $FMNH_2$ reduction catalyzes with the assistance of NADPH and molecular oxygen [19-22]. Aeration facilitates diminish product-inhibition circumstances that appeared during the anaerobic growth by organic acid secretion [23, 24].

Oily sludge as an environmental challenge could be a substituted complex carbon source for microbial cobalamin production. From the reservoir to the refinery sections, based on leakage or as the by-product of unit operations, oily sludge is produced [25]. Many attempts have been accomplished to treat such kinds of sludge in order to improve the environmental criteria compatibility of the oil industry [26, 27]. Among all introduced methods for the oily sludge treatment, bioremediation also has been considered [28, 29]. It has been shown that pure and sole bacteria culture could degrade the oily sludge as well as a designed consortium of the bacteria. Cobalamin producing bacteria like *Bacillus megaterium* has degraded the oily sludge of the petroleum industry solely and in the synthetic mixed culture [30]. Biodegradability of the petroleum hydrocarbons decreases from n-aliphatic to complex multi aromatic cycles and asphaltenes, respectively. The presence of *Propionibacterium* in crude oil has been reported by some researchers [31].

Aeration is a vital step in synthesizing the active form of cobalamin, due to the molecular oxygen effect on the DMBI production [19], and any phenomenon like introducing the nanoparticles (NPs) to the system which could modify the oxygen transfer rate, would be considerable.

Nanotechnology, the knowledge of using the benefit of nanometer scales, nowadays has widely spread in so many subjects of the science [32, 33]. Many applications for nanoparticles and Nano-fluids have been explained [34]. Al_2O_3, SiO_2, TiO_2, CNT (carbon Nano-tube), Fe_2O_3, and Fe_3O_4 nanoparticles have caused gas-liquid mass transfer modification. Fe_2O_3 and Fe_3O_4 have been applied to enhance the oxygen delivery to the biomass in the fermentation process [35, 36]. The volumetric mass transfer coefficient of a liquid phase, $\boldsymbol{K_L a}$, has increased by adding the magnetite NPs to the fermentation [37]. Shuttle impact, boundary layer complexing, and Prevention of gas-phase fragments coalescence are the three leading mechanisms of mass transfer coefficients modification of the NPs incorporation [38].

In the present study, magnetite NPs synthesis and microbial cobalamin production with NPs assistance have been assessed. Since the applied

NPs synthesis method in our work was a little bit different from the others, complete characterization procedures were employed. We have used oily sludge (supplied from Iranian group one base oil production refinery) as the sole carbon source for the fermentation of *P. freudenreichii* while the Fe_3O_4 NPs have been introduced to the culturing medium in the second half of the process. Response to surface methodology (RSM) has been applied as the statistical analysis on both parts of this work.

MATERIAL AND METHOD

Chemicals and microorganism

Microorganism

High G+C bacteria, *Propionibacterium freudenreichii subsp. freudenreichii* PTCC1674 (*P. freudenreichii*) has been procured from an Iranian research organization for science and technology subsidiary; Persian type culture collection (PTCC) in the form of live culture. Based on the PTCC database, the solid culture was prepared on sodium lactate agar. Reserve bacteria collection on the recommended *propionibacterium* solid agar was cultured as the live culture arrived in our laboratory.

chemicals and reagents

chemicals for magnetite NPs synthesis

Iron powder (abcr GmbH), hydrochloric acid HCl solution 35% (LAB-SCAN), ammonium hydroxide, ammonium hydroxide 28-30%,(lach: ner), argon gas were purchased via commercial sources and used directly without further purification, distilled water and acetone were used for washing of synthesized samples.

Chemicals for cobalamin production

bacteriological agar, glucose, peptone casein, yeast extract were purchased from Merck (Darmstadt, Germany), sodium lactate 60%, Cyanocobalamin (Vitamin B12), betaine hydrochloride from Sigma-Aldrich (Germany), L-glutamic acid, cobalt chloride supplied from Sam Chun (Seoul, S. Korea), 5,6 dimethyl benzimidazole, magnesium chloride, manganese chloride, tripotassium phosphate, monopotassium phosphate, sodium dihydrogen phosphate, sodium chloride, zinc chloride, ferrous sulfate heptahydrate, calcium chloride, calcium carbonate, Di-ammonium phosphate, provided from Merck (Germany). Oily sludge supplied from Iranian group one base oil refinery.

Magnetite NPs synthesis

A range of methods has been investigated to produce Fe_3O_4 nanoparticles. From coprecipitation, solvothermal, thermal decomposition up to production via magnetotactic bacteria were mentioned as the Fe_3O_4 NPs synthesis routs [35]. The most common method for this nanoparticle production is coprecipitation of ferrous and ferric chlorides using alkali like NH_4OH or NaOH. Of course, sometimes, $FeCl_2$ has been replaced by $FeSO_4$ [39]. As the acquiring of $FeCl_2$ and $FeCl_3$ needs pre-curation of iron, it has been proposed a method of magnetite NPs synthesis from iron sands [40]. In this work, we have used the method developed by Gunanto et al., and Simamora et al., with some alteration [40, 41]. In the first step, the Iron powder (instead of iron sand) was dissolved in HCl at 80°C with a constant agitation rate of 700 rpm. The obtained iron chloride solution, $FeCl_x$, is then slowly etched with NH_4OH 28% while being heated to the temperature of trials with a regular stirrer rate to obtain black precipitates. Reaction time, temperature, and agitation speed are the subject of statistical optimization, which were varying over the designed ranges in the following. All the experiments were done under positive argon gas pressure avoiding NPs post-synthesis reactions. The resulting precipitates were then magnetically collected and washed repeatedly with distilled water and acetone to remove residual material to reach the neutral pH for further characterizations. Because of the stability of the nanoparticles, it is better to keep the synthesized NPs in the form of Nano-fluid suspension to utilize by the fermentation part of the study.

magnetite NPs characterization

Since we have executed some alteration to the reported method of Fe3O4 NPs production and to understand the properties of the nanoparticle additive of the fermentation part, it is obligated to follow the characterization procedures of the obtained nanoparticles.

X-ray diffraction analysis

Structural analysis of the materials has been analyzed by using X-beam irradiation. The synthesized Fe_3O_4 samples were determined by Powder X-ray Diffraction (PXRD) experiments. X-ray diffraction data were collected on a RIGAKU SmartLab 3 kW diffractometer with a fine focus Cu sealed tube with graphite monochromated

MoKα at 40 kV, 30 mA. Sample height was aligned with laser, and data were collected for the desired range. Samples were pressed on an aluminum slide, and data were recorded from 15<2θ<60 degrees. Simulated powder patterns from single-crystal X-ray diffraction data were generated using Mercury software. X-ray beam irradiated to the sample and scattered from NPs based on their crystallography diffraction properties. The detector is moved around the sample on the circular pattern while the x-ray intensity is recorded in the unit of counts or counts per second in each position (2θ).

Scanning electron microscopy (SEM) analysis

For the morphological investigation of the Synthesized NPs and particle size assessment, we have used the field-emission scanning electron microscope (SEM, JEOL JSM 7500F, FEI Verios 460L) in this study. FE-SEM has been widely used for nanoparticle analysis. The electron beam emitted from the generator and based on the interaction between contacted electrons and the specimen surface, a magnified image of the particles is constructed. The shape of Fe_3O_4 NPs has been characterized via FE-SEM while the particle size obtained by ImageJ application (image processing package) assistance.

Energy Dispersive Spectroscopy (EDS)

EDS or energy-dispersive x-ray spectroscopy is a coupled module with the SEM to generate the quantitative elemental results of observed nanoparticles or any specimen. During electron beam emission to SEM image obtaining, a range of signals is generated. X-ray is one of those mentioned signals which is uniquely related to the element which is producing the signal. Each element radiates its specific x-ray signal from the energy aspect. It means every element in the composition of nanoparticles, yields a specific pick in the EDS or EDAX spectra. We have used such kind of analysis to check the Fe_3O_4 NPs to ensure and investigate the molecular composition of the synthesized NPs.

microbial cobalamin synthesis

Inoculum preparation

The pre-culture medium constituents were: 20 $g.L^{-1}$ glucose, 5 $g.L^{-1}$ peptone, 10 $g.L^{-1}$ yeast extract, 2 $g.L^{-1}$ KH_2PO_4, 5 $g.L^{-1}$ di-ammonium phosphate, and pH of the medium was turned to 7, using proper alkali solution. At least 3 flasks with 150 ml working volume with the above composition prepared and placed in the anaerobic jar which is N_2 gas has been purged in to obtain the anaerobic situation. *P. freudenreichii* cell colonies were transferred into a couple of flasks, and one of them was kept as the blank control. Afterward, the anaerobic jar was positioned in the shaker incubator with 150 rpm agitation speed at 30°C. Twenty-four hours left the system in the mentioned condition to pass the log-phase of *P. freudenreichii* growth.

Cobalamin synthesis investigations

DMBI and NPs effect comparison on cobalamin production

We have just organized 4 trials in this part of the study to compare NPs presence and DMBI incorporation effects on the cobalamin production. The sole carbon source in these four experiments is the glucose of 30 $g.L^{-1}$ and NPs suspension added by 4% v/v at the smallest mean size which is obtained from the previous section of the present work, and the working temperature was 35°C. The other components of the culturing medium and aerobic and anaerobic fermentation plan will be the same as the next part.

Cobalamin synthesis and optimization

In this part, initially, we prepared a mixture of oily sludge in 100 ml deionized water. As the percentage of the oily sludge was proposed by the experimental design procedure, the recommended amount of sludge weighted and poured in the water. Afterward, the mixture was put under ultrasonic irradiation (50 w for 5 minutes),. Then all the mixture was centrifuged at 1000 rpm for 10 min to separate solid components of the sludge. The supernatant introduced to the fermentation flasks and other components of the medium will be added in this stage. Oily sludge as the carbon source, percentage of added NPs suspension to the culturing medium, and the temperature of the fermentation was designed by the statistical experimental design procedure. All the other ingredients composition in the culturing media is as follow 2 $mg.L^{-1}$ zinc chloride, 20 $mg.L^{-1}$ ferrous sulfate, 20 $mg.L^{-1}$ magnesium chloride, 4 $mg.L^{-1}$ cobalt chloride, 2 $mg.L^{-1}$ calcium chloride, added to the system for the trace element supplementation. 10 $g.L^{-1}$ peptone casein, 10 $g.L^{-1}$ yeast extract, 0.2% w/v L-glutamic acid, 10 $g.L^{-1}$ diammonium hydrogen phosphate, 1 $g.L^{-1}$ betaine hydrochloride were added to the fermentation flask to supply

the main components. The working volume of Culturing mediums increased to 150 ml then autoclaved and 10% v/v inoculum medium added to them. All the experiments were implemented under the anaerobic condition for 3 days and aerobic situation for the other 3 days consecutively. The pH adjusted between 6.8-7. Whenever NPs suspension incorporation to the culturing medium has been planned, it has been added at the beginning of the aeration step of the fermentation attempts (second 3 days).

Cobalamin extraction and quantification

At the end of 6 days (144 hours) anaerobic and aerobic fermentation, it is highly recommended to convert all the methyl, hydroxyl, and adenosyl form of cobalamin to the cyanide form as the most stable cobalamin in the extracellular condition. 40 ml of the fermentation broth centrifuged for 15 minutes at refrigerator temperature (4°C), under 8000 gravitational force (g). Then supernatant removed and cellular pellets resuspended in phosphate buffer of pH=5.5 (0.2 M). This step was repeated twice and at the end of the second course of washing, pellets dispersed in phosphate buffer containing 0.1% w/v KCN. Cellular suspension boiled for 30 minutes to ensure extraction of cobalamins and complete conversion to the cyanide form. After cooling, the cellular mixture centrifuge with the conditions as mentioned above to discard the cellular pellets. Then the supernatant was filtered by a 0.45 nm syringe filter and introduced to high-performance liquid chromatography (HPLC) analysis. HPLC system (Smartline KNAUER 2300-Germany) using a UV detector at 361 nm applied to quantify produced cyanocobalamins. In this study, a reversed phased Eurosphere C18 column (250 mm×4.6 mm, 5μm) was installed. The elution protocol was in the linear gradient format of 15:85 - 50:50 % v/v methanol-water as the mobile phase. The duration of the HPLC cycle was 25 minutes [42].

statistical design of experiments

Response surface methodology (RSM) is the parametric statistical approach including sort of experimental trials scenario recommendation, fitted model extracting, and eventually implementing response optimization. Analysis of variance (ANOVA) is the core of this method to investigate the grouped results and verification the statistical hypothesis.

Box-Behnken design for magnetite NPs synthesis investigation

Box-Behnken design (BBD) is applied to statistically investigate the quadratic model of variables with three levels; upper, lower, and center. BBD has used the incomplete factorial design to draw the scheme of trials. All the trials number is $2F(F-1)+C$, which F is the number of independent factors, and C is the number of center points. In this study, we have planned the BBD scheme of experiments with 13 trials, including one center point. Regarding the literature review, we have chosen the synthesis temperature of 60-80 °C, reaction duration (Time) of 10-30 minutes, and reaction medium agitation speed (Turbulency) 600-800 rpm as the independent variables.

Central composite design (CCD) for microbial cobalamin production investigation

Central composite design (CCD) considers out of the defined range of independent variables for statistical assessment based on selected distance from the central point (α). It is practical to define α between 1 and $\sqrt[4]{2^F}\sqrt[4]{2^F}$ that F is the number of independent variables. The total number of CCD trials are 2^F+2F+C. C is the number of center point replicates. In this study, we have chosen the CCD scheme of experiments with 18 trials carrying four replicates of a center point. Three parameters including; oily sludge of 1-6 % w/v as the sole carbon source, incorporation of magnetite NPs suspension of 4-8 % v/v, and fermentation temperature of 30-40 °C were assessed through CCD analysis. In this work, Applied α was 1.31607. All the RSM attempts have been made by Design Expert.10 software.

RESULTS AND DISCUSSION

Fe_3O_4 NPs synthesis

It is essential to obtain what kind of parameters can influentially affect the size of synthesized NPs. In this part of our work, BBD recommendations have been followed to address the effect of variables on the size of NPs as the response.

Table 1 shows the criteria of all trials and the obtained size of NPs as well as the polydispersity index (PdI) of each attempt. We have calculated PdI from its equality with the square of (standard deviation over the mean particle size). As explained in section 2.3.2, by applying image processing software (ImageJ), the distribution of the particle size data has been extracted. Then, through the

Table 1. BBD results and designation for NPs production.

Std	Run	Temp (°C)	Time (min)	Turbulency (rpm)	Size of NPs (nm)	Standard Deviation (sd)	Pdi= $(\sigma/d)^2$
13	1	70	20	700	21.55	3.08	0.020
12	2	70	30	800	24.33	5.56	0.052
6	3	80	20	600	44.1	7.27	0.027
4	4	80	30	700	50.1	6.65	0.018
1	5	60	10	700	13.86	1.66	0.014
10	6	70	30	600	30.1	4.57	0.023
5	7	60	20	600	17.97	2.53	0.020
11	8	70	10	800	21.53	4.76	0.049
7	9	60	20	800	16.74	2.62	0.025
9	10	70	10	600	20.63	3.32	0.026
3	11	60	30	700	19.24	3.27	0.029
2	12	80	10	700	31.83	5.14	2
8	13	80	20	800	31.7	4.83	0.023

histogram graph analysis with Origin Pro. (2016), the proper Gaussian function was fitted. Hence, the mean size of NPs and the standard deviation (sd) was achieved. Fig .1 illustrates the particle size distribution of 3 selected runs. Although the particle size is the essential parameter for focusing during NPs synthesis, the PdI investigation is a vital challenge. Producing the monodisperse bunch of NPs guarantees the properties which are expected from NPs using in a system. There is no PdI more than 0.1; it means that the designed experiments resulted in monodisperse particles as well as quite enough small size.

In our 13 trials, the smallest mean size was around 14 nm with PdI=0.014 produced by run order number 5 and the biggest one was about 50 nm with PdI=0.018 based on run order number 4. As the RSM statistical analysis is the parametric assessment model; the data collection has to have a normal distribution. Unfortunately, some studies, without considering this principle, proceed to the next steps. It is obligated to show our data normality, and it has been shown in Fig. 2. In the normal plot of residues, the data should distribute close to the 45-degree baseline, which proves the normality of the results. Based on lambda=1 represented by Box-Cox assessment (not shown), there is no need for executing of exponential or power-law transformation to normalize obtained results for further studies.

ANOVA of the quadratic fitted model (R^2=0.9763, R^2_adj=0.9052) of our study has reflected the model *p*-value less than 0.05 (Table 2). Therefore, the model correlation was significant, and based on this model, the effect of each factor individually, or interaction effects of the parameters could be analyzed. It is acceptable to take into account the *p*-value threshold of 0.1, and on this basis, the direct effect of time (A) and reaction temperature (B) and pure quadratic effect of time (A^2) are statistically significant. The direct effect of turbulency (C), the interaction effect of time and reaction temperature (AB), the interaction effect of time and medium turbulency (AC) are considered

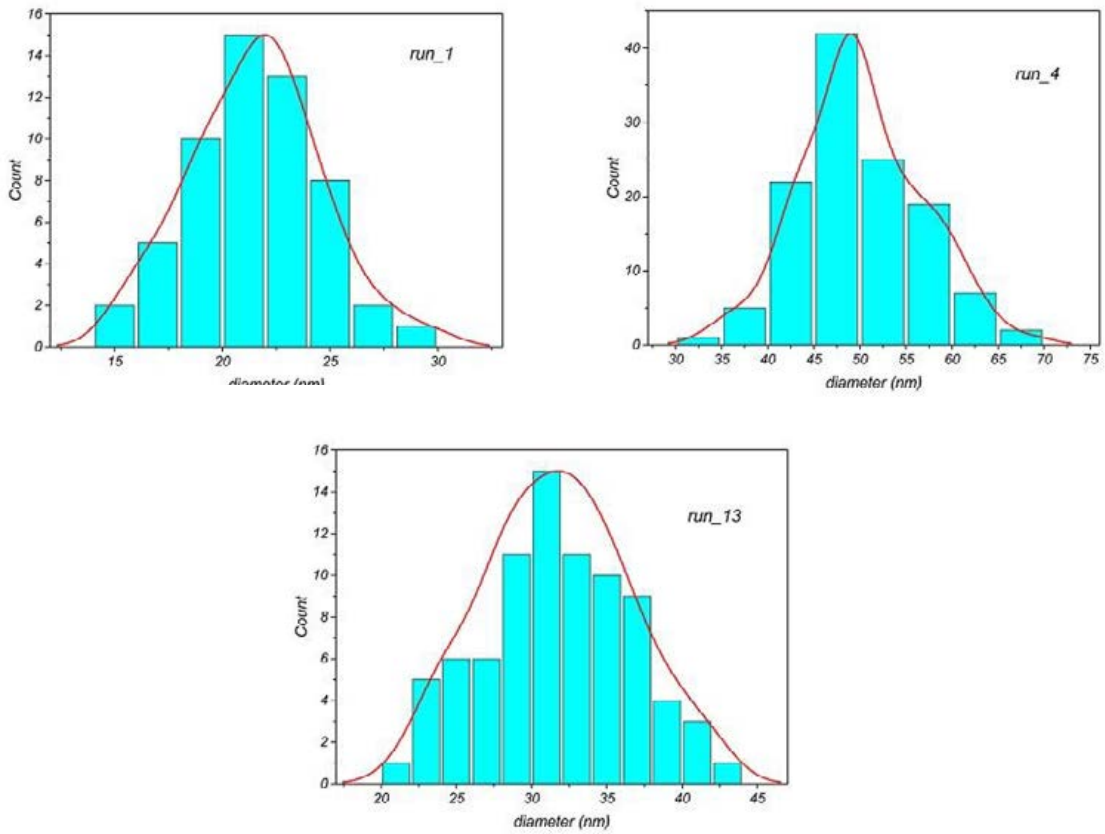

Fig.1. histogram plots of a) run_1, b) run_4, c) run_13 that reflect the mean size and size dispersity of synthesized Fe_3O_4 NPs.

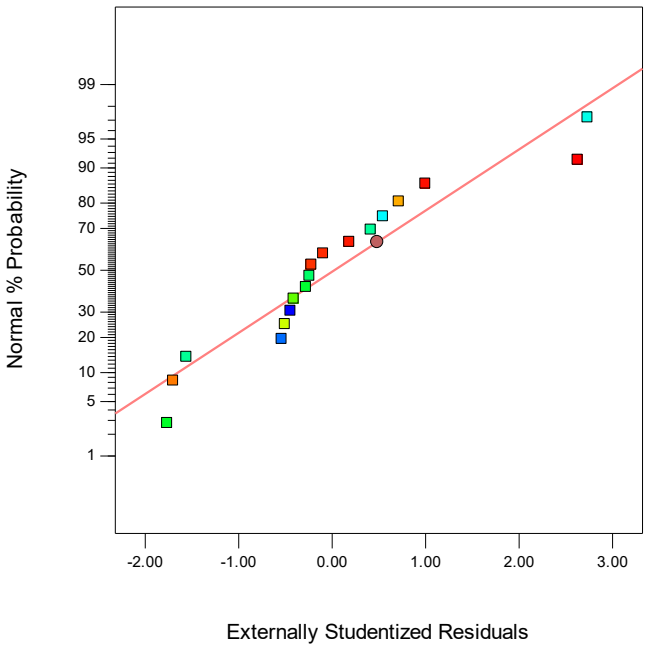

Fig. 2. Normal plot of residuals for NPs synthesis by BBD method.

Table 2. ANOVA outcomes of Box-Behnken design of RSM study for magnetite NPs synthesis.

Analysis of variance table (ANOVA) for Fe3O4 NPs synthesis by BBD method					
Source	Sum of Squares	df	Mean of Square	F Value	p-value
Model	1370.67	9	152.30	13.73	0.0269
A-Temp	1010.70	1	1010.70	91.14	0.0024
B-Time	161.28	1	161.28	14.54	0.0317
C-Turbulency	42.78	1	42.78	3.86	0.1443
AB	41.54	1	41.54	3.75	0.1484
AC	31.19	1	31.19	2.81	0.1921
BC	11.12	1	11.12	1.00	0.3904
A^2	65.27	1	65.27	5.89	0.0937
B^2	7.94	1	7.94	0.72	0.4596
C^2	1.23	1	1.23	0.11	0.7610
Residual	33.27	3	11.09		
Cor Total	1403.94	12			

for future studies however, they are not statistically significant. Equation 1 shows the mathematical relationship between the variables and their interactions, on the synthesized Fe_3O_4 NPs size.

Equation 1:

Size of NPs = +21.55 +11.24 * A +4.49 * B -2.31 * C +3.22 * AB -2.79 * AC -1.67 * BC +5.34 * A^2 +1.86 * B^2 +0.73 * C^2Due to the above equation, main effect plots and interaction plots which are produced by our BBD analysis, temperature, and reaction time have a direct effect on the response (particle size). By the increase of temperature, the particle size increased. Besides, by lasting the reaction time, the particle size went up. From temperature to turbulency, the slope of the effect of parameters reduced, while the slope of the turbulency turned to the small negative amounts. We have found out; the reaction temperature is the most influential parameter. After that, the reaction time has a significant effect on the NPs size. Among the interaction effect of parameters, the temperature-time interaction was the greatest, and they show their synergistic effect in the results that appeared in Table 1.

Karade et al. (2018), studied the effect of reaction time on the magnetic NPs synthesis [43]. They claim that the reaction time growing caused to bigger particle size; however, the crystallinity is also improving. Hernandez et al. (2018), introduced the holding time and show that the reaction time has a direct effect on the increase of the Fe_3O_4 NPs even through the solvothermal method [44]. The temperature of the synthesis reaction appeared as the most crucial parameter in the other studies as well. Temperature is highly affecting the nucleation and agglomeration of particles. The coprecipitation method is the combination of nucleation of the core crystals and growing simultaneously. During the nucleation, small size particles are constructed while during the growing phase, the agglomeration happens. Cushing et al. (2004), highlighted the growing part of the coprecipitation as a reaction analogy and they have proved that the variables like temperature and agitation of the medium, which are affecting the reaction rates, can alter the size of synthesized particles [45]. Rahmawati et al. (2017), experienced that the agitation speed of the reaction media inversely influenced the particle size of NPs. Of course, its effect is not substantial [46]. Our findings on the synthesis of the Fe_3O_4 NPs well described that the new recommended procedure is working properly. Fig.3 draws the RSM surface and contour graphs. As it is apparent in all images of Fig. 3, there is no local extremum, and the maximum and minimum are located at the edge of our design. Therefore, the result of optimization conforms to the smallest size of NPs, which is obtained from the BBD study. The smallest size of 13.86 nm was afforded at the synthesis temperature of 60 °C, reaction duration of 10 minutes, and the medium turbulency of 700 rpm. The NPs suspensions were prepared in addition to the fermentation part of our study based on the smallest obtained particle size in this part of our work.

characterization of the synthesized NPs

Since we did not use the prepared Fe^{2+} and Fe^{3+} carrying molecules, such as $FeCl_3$ and $FeCl_2$ or $FeSO_4$, to Fe_3O_4 NPs synthesis; it is vital to implement the characterization tests. SEM images

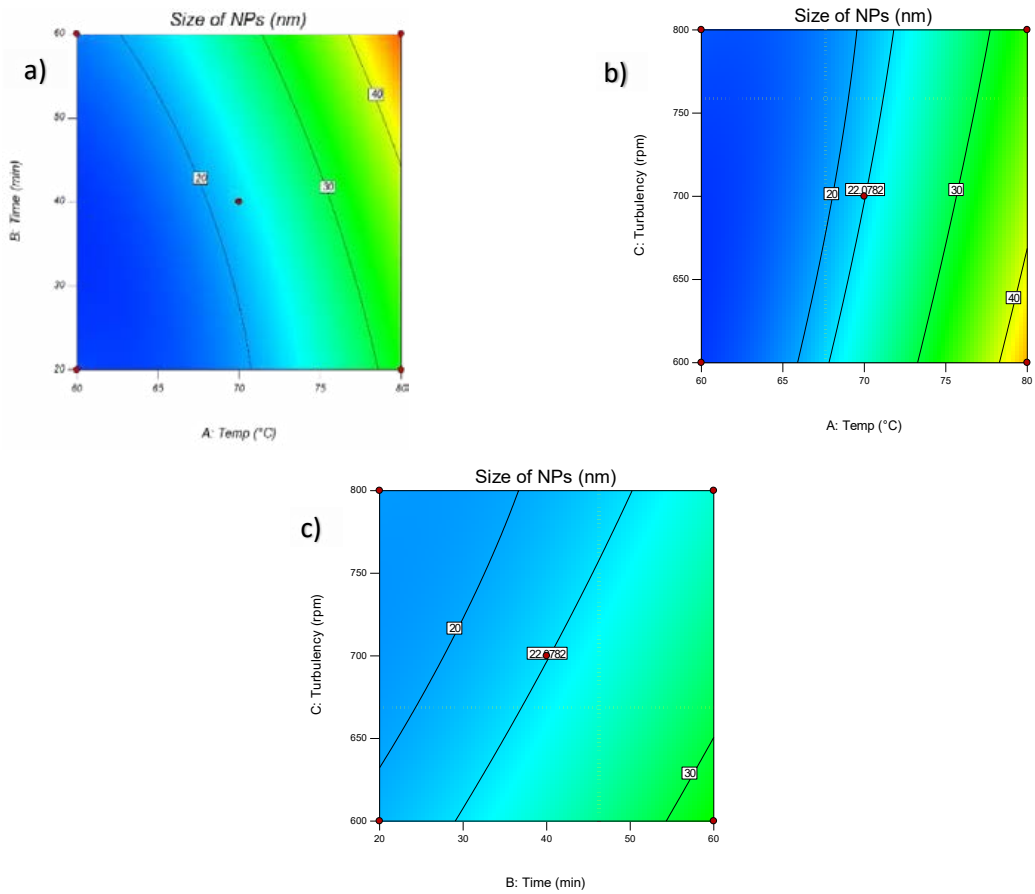

Fig. 3. Effect of investigated parameters on Fe_3O_4 NPs synthesis production by BBD method. a) reaction time and temperature interactions, b) turbulency and temperature interactions, c) turbulency and reaction time interactions.

of synthesized Fe_3O_4 samples are shown in Fig. 4. In some pictures, agglomeration was observed, and it can be associated with a high magnetic saturation of the NPs. A homogeneous distribution has been figured, with an apparent particle size between 10 to 70 nm. Also, from SEM analysis, it was possible to determine that the synthesized NPs have cubic to spherical shape.

Elemental analysis of the synthesized NPs, which was accompanied to show the Fe/O weight portion, conforms to the Fe_3O_4 atomistic portion of 2.62. The elemental components of the synthesized compound were determined by the EDS module. According to the obtained spectrum, Fig. 5, Fe and O distributions were 39.33% and 51.8%, respectively (Table 3) which confirm the formation of Fe_3O_4 particles nicely. Cl and C were also present, which are related to unreacted FeCl and coating material, respectively. The Fe/O portion obtained from weight% and atomic% (multiplied to molecular weights) is 2.69 and 2.65 that confirm the Fe_3O_4 molecular structure.

Fig. 6 shows the PXRD patterns of run_1, run_4, run_13 samples, and also the simulation pattern of Fe_3O_4. Comparison and study of the PXRD patterns of the synthesized samples and simulation one show that the diffraction lines corresponding to the (111), (220), (311), (400), (442), and (511) lattice planes for these materials appear at the same 2 theta angles. It proves that the synthesized samples have the same inverse spinel structure that we expect from Fe_3O_4. No other phase impurity peaks were observed, indicating the successful synthesis of pure magnetite Fe_3O_4 NPs.

DMBI and NPs effect comparison on cobalamin production

As the diary *propionibacterium* species are generally recognized as the safe (GRAS) species, vitamin B12 (Cyano-Cbl) production by such

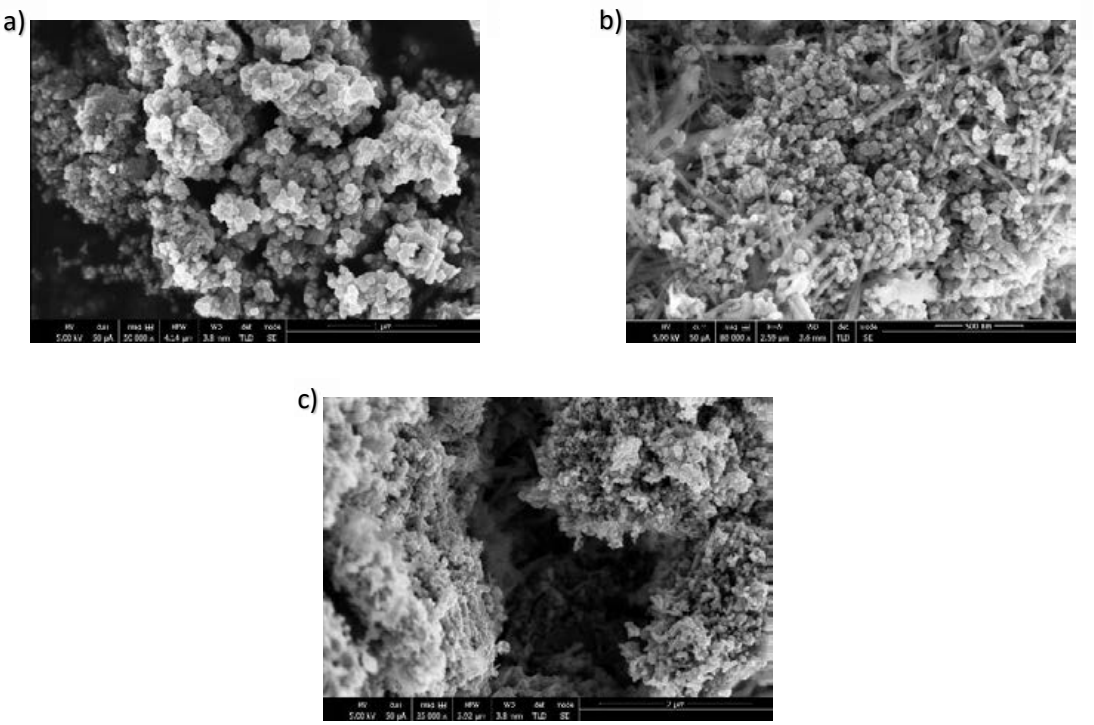

Fig. 4. The SEM image and morphology analysis of a) run_1, b) run_4, c) run_13.

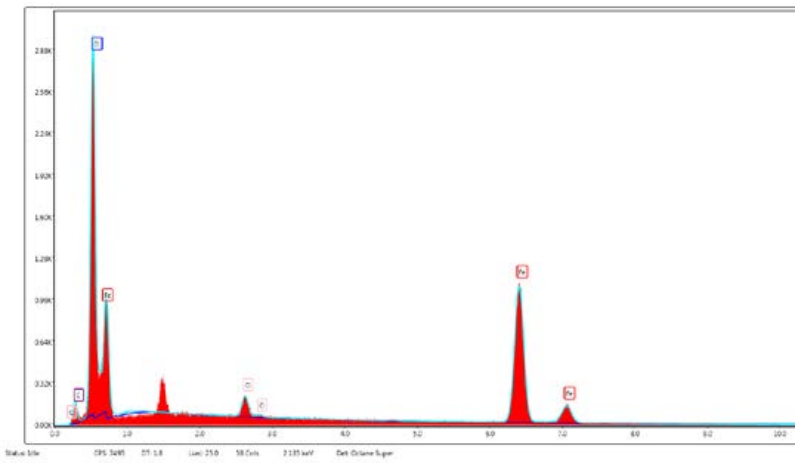

Fig. 5. EDAX spectra, which draws the elemental composition of synthesized NPs.

Table 3. elemental percentage of synthesized NPs extracted from EDS analysis.

Element	Weight %	Atomic %	Error %	Net Int.	P/B Ratio	R	F
C K	2.66	7.02	16.99	100.84	0	1	1
O K	26.1	51.8	15.47	1801.63	0	1	1
Cl K	2.07	1.85	13.8	141.5	15.5968	1.0283	1.0303
Fe K	69.18	39.33	3.88	1324.16	459.701	1.0466	1.0271

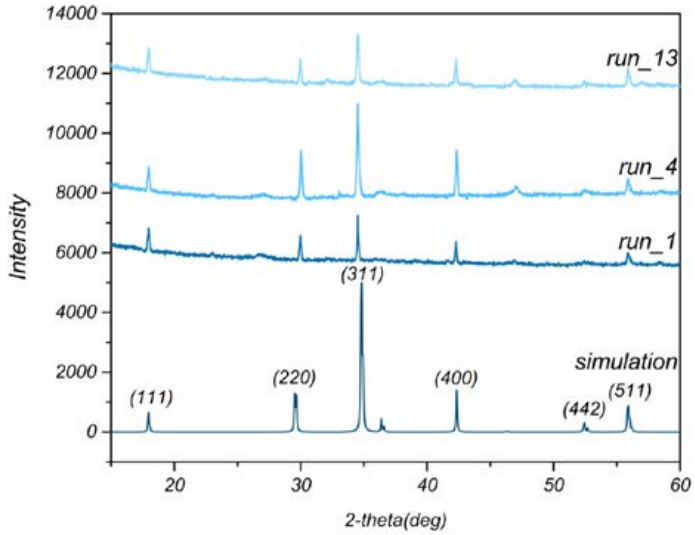

Fig. 6. PXRD pattern of run_1, run_4, run_13, and simulated reference of Fe_3O_4 NPs synthesized by BBD method.

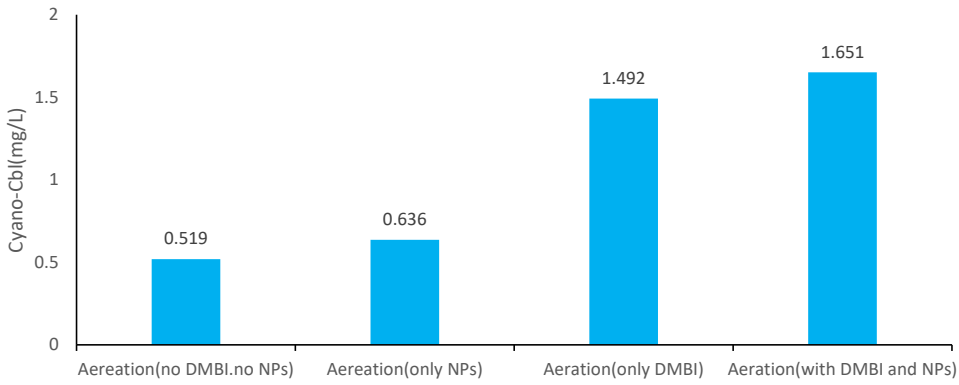

Fig. 7. The comparison of NPs addition and DMBI presence in the fermentation medium. The carbon source of these experiments is glucose.

strain increasingly has been considered. In Fig.7, we have compared the DMBI addition effect vs NPs addition effect on the cobalamin production. As explained before, *P. freudenreichii* is an anaerobic aerotolerant prokaryote bacteria. The primary role, which is assigned to its aeration, is participating in the DMBI synthesis pathway. Since both (DMBI and O_2) have the same action route, they have been compared in the present study. As it is obvious, NPs addition to the fermentation system can slightly improve the cobalamin production, but DMBI still has a more considerable effect on the cobalamin synthesis. The NPs can improve the gas-liquid mass transfer, Fig. 7 has addressed it and most probably higher delivered and uptake oxygen should be participated in the DMBI and eventually cobalamin synthesis pathway. The NPs incorporation could improve around 20% of Cyano-Cbl production; however, DMBI has increased the obtained cobalamin about 3 fold. The NPs addition didn't have an impressible impact on the cobalamin production in the medium containing DMBI. Among many strategies for Cyano-Cbl modified production, Wang et al. (2015), have also shown the DMBI addition and its time of incorporation to the fermentation medium is the most effective impact [54]. Nonetheless, we try not to use the DMBI in cobalamin production in the next part. We benefit from NPs using, and O_2 modified transferring to produce the Cyano-Cbl in the following.

Table 4. CCD results and designation for Cyano-Cbl production.

CCD experiments and results					
Std	Run	A:oily sludge (% w/v)	B:NPs (% v/v)	C:Temp (°C)	Cyano-Cbl (mg/L)
7	1	1	8	40	0.926
12	2	3.5	8.63215	35	1.497
15	3	3.5	6	35	1.459
6	4	6	4	40	1.074
3	5	1	8	30	0.541
5	6	1	4	40	0.809
11	7	3.5	3.36785	35	1.328
14	8	3.5	6	41.5804	1.511
1	9	1	4	30	0.424
17	10	3.5	6	35	1.467
10	11	6.79019	6	35	0.916
13	12	3.5	6	28.4196	0.857
9	13	0.209815	6	35	0.721
4	14	6	8	30	0.8034
16	15	3.5	6	35	1.485
18	16	3.5	6	35	1.381
2	17	6	4	30	0.691
8	18	6	8	40	1.189

Cobalamin synthesis and optimization

In this part of our work, cobalamin production from oily sludge was targeted. Three parameters including oily sludge as the sole carbon source, incorporation of magnetite NPs suspension, and fermentation temperature were assessed through CCD analysis for cobalamin synthesis investigation. Since the *P. freudenreichii* is a propionic acid and acetic acid producer, pH decrease at the end of the anaerobic step shows the microbial growth on the newly selected carbon source. Of course, the collected cobalamin at the end of the aerobic step confirms the microbial growth as well.

Table 4 indicates the parameter levels, designed experiments, and the obtained results. The outcomes vary between 0.424-1.511 $mg.L^{-1}$ of Cyano-Cbl. It has shown a new carbon source for *P. freudenreichii* however, it was figured out that this strain can grow on the kerosene (a fraction of crude oil) while producing cobalamins [47]. We have followed all the necessary criteria for a well-done RSM analysis, and the illustration of the ANOVA assessment appeared in Table 5.

The represented model was significantly fitted to the obtained result of experiments (R^2=0.98, adj-R^2=0.96). Duo to the contour plots denoted in Fig. 8, oily sludge effect on the cobalamin production reflects the local maximums in its specified interval; it means by the increase of the oily sludge portion, growth inhibition would be possible that could be categorized as the substrate inhibitions. It has been proved that the facultative anaerobe bacteria, which demonstrates nitrate reductase activity, can degrade the hydrocarbon compounds [48]. Also, it was described, the bacteria which is producing biosurfactants can more efficiently utilize the hydrocarbon substrates [49]. *P. freudenreichii* shows the nitrate reductase activity, and Hajfarajollah et al. (2014), have experienced the biosurfactant production in this strain [50]. On

Table 5. ANOVA outcomes of central composite design of RSM study for Cyano-Cbl production.

Analysis of variance table (ANOVA) for Cyano-Cbl production by CCD method					
Source	Sum of Squares	DF	Mean of Square	F-Value	p-value
Model	2.19	9	0.24	53.16	0.0001
A-oily sludge	0.15	1	0.15	32.92	0.0004
B-NPs	0.041	1	0.041	8.92	0.0174
C-Temp	0.5	1	0.5	109.76	0.0001
AB	5.45E-06	1	5.45E-06	1.19E-03	0.9733
AC	2.45E-07	1	2.45E-07	5.36E-05	0.9943
BC	8.45E-07	1	8.45E-07	1.85E-04	0.9895
A2	1.06	1	1.06	230.72	0.0001
B2	0.022	1	0.022	4.83	0.0593
C2	0.24	1	0.24	51.76	0.0001
Residual	0.037	8	4.58E-03		
Lack of Fit	0.03	5	6.05E-03	2.86	0.2078
Pure Error	6.34E-03	3	2.11E-03		
Cor Total	2.23	17			

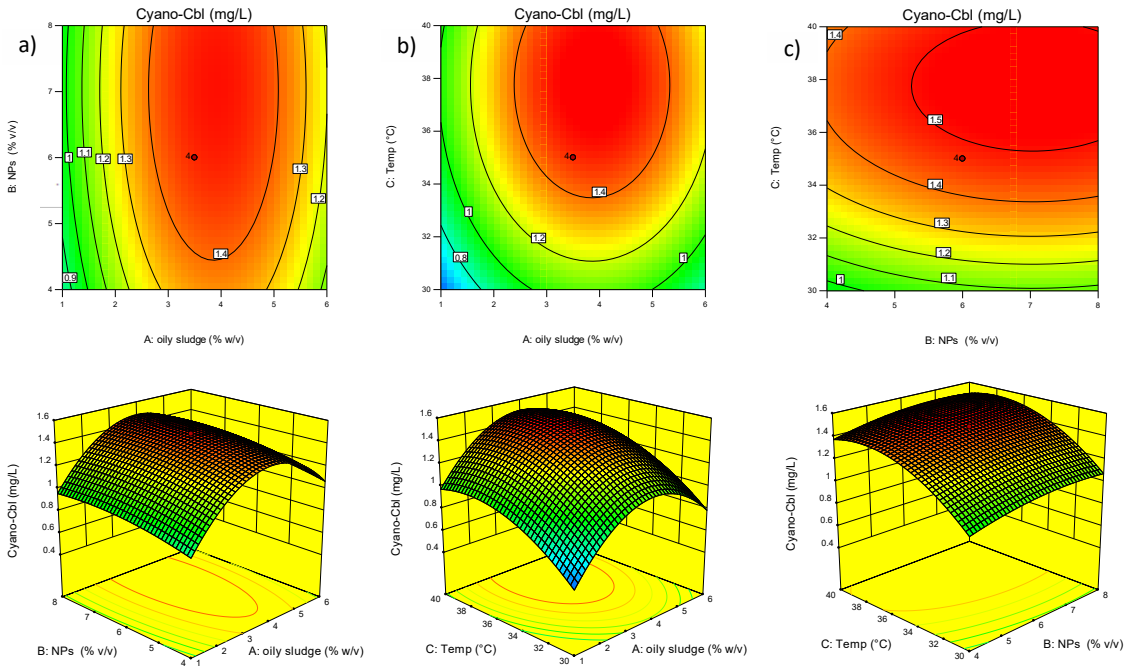

Fig. 8. Effect of investigated parameter on Cyano-Cbl production by CCD method. a) Oily sludge and NPs interactions, b) Oily sludge and Temperature interactions, c) NPs and Temperature interactions.

that basis, we have selected such culturing medium designation. The other finding of this study was how NPs incorporation could affect cobalamin production. The effect of NPs addition as a mass transfer enhancer has been a disputed subject. On one hand, it is widely accepted that the aeration after

anaerobic fermentation can improve the cobalamin production yield. On the other hand, toxic oxygen levels and growth inhibition through increased K_La are substantial factors. In the older case, it has been expressed that the *propionibacterium* culture uptakes all the available oxygen in the lower K_La**=10** hr^{-1} [51]**.** But**,** in the higher volumetric mass transfer coefficients, this strain cannot grow even in the anaerobic conditions. Of course, their study was in the continuous form, and it seems oxygen concentration escalation via the increase of K_La could not be comparable with the works under surface aeration culturing. A little later, Quesada-chanto et al. (1998), have demonstrated that this strain can grow even up to K_La**=53** hr^{-1}. They had obtained cobalamin production reduced when mass transfer coefficient increased [52]. Of course, they didn't execute any anaerobic growth phase before aeration culturing, and their finding completely fair because, without the anaerobic section, cobalamin precursors could not be synthesized. Eventually, Galacton et al. (2005), have mentioned the amount of desire effect of K_La increase strictly depends on the bioreactor and broth conditions [53]. In our work, the effect of NPs addition follows a slightly positive impact on the cobalamin production in its defined range of action. Nevertheless, it has to be considered that the water solubility decreases considerably from 30°C to 40°C. It seems the greater volumetric mass transfer coefficient has compensated for the appeared oxygen shortage based on NPs incorporation into the system. The other point is substrates like oily sludge are the harmful component for the mass transfer phenomena. Labbeiki et al. (2014), calculated the 2 %v/v magnetite NPs suspension addition to the deionized water caused to K_La of 5.862 hr^{-1}. Such a magnitude of K_La and even higher amounts are in favor of *propionibacterium* growth and bioproducts formation. The temperature has a synergistic effect in combination with two other factors.

Equation 2 expresses the mathematical correlation between the response and independent variables. The software recommended the optimized condition at oily sludge of 4 %w/v, NPs suspension of 7.5 %v/v, and 37°C to obtain 1.548 $mg.L^{-1}$ of Cyano-Cbl. We have planed the condition and reached 1.537 $mg.L^{-1}$ of response.

Equation 2 :

$$\text{Cyano-Cbl} = +1.47 +0.11 * A +0.06 * B +0.21 * C -8.25E\text{-}004 * AB -1.75E\text{-}004 * AC +3.25E\text{-}004 * BC -0.40 * A^2 -0.058 * B^2 -0.19 * C^2$$

CONCLUSION

We have produced, characterized, and optimized Fe_3O_4 NPs from iron powder through the coprecipitation method. The smallest obtained mean size was 13.86 nm. The morphological analysis via SEM image, structural assessment by PXRD investigations, and composition analysis through EDS spectra, all confirmed the proper production of NPs. Box-Behnken design method has been acquired for the statistical examination of this part of the study, and it was an appropriate solution for a brief and comprehensive analysis for NPs synthesis. Afterward, two-step fermentation (anaerobic and aerobic) has been executed to study the cobalamin production. In most of the studies using the exogenous DMBI to a biologically active form of cobalamin synthesis, we have chosen the efficient aeration step by NPs incorporation instead of DMBI addition. The effect of NPs addition and DMBI presence on the microbial cobalamin production was investigated. The positive impact of NPs incorporation was extracted; however, DMBI presence, still has the dominant effect on Cyano-Cbl production. In the last part of our work, Cyano-Cbl production has been investigated and optimized through the Central Composite design method. Oily sludge concentration, NPs portion, and the temperature were the studied parameters. The effect of oily sludge shows the local maximums. NPs addition effect needs more studies because of the controversial effect of temperature increase and NPs addition on the volumetric mass transfer coefficient and oxygen solubility.

ACKNOWLEDGMENT

This work was supported by the Babol Noshirvani University of Technology research grant no: BNUT/925150010/99. Many thanks to the Biotechnology Research Lab at Babol Noshirvani University of Technology (BNUT), Babol, Iran, for all cooperation.

CONFLICT OF INTEREST

The authors declare that they have no conflict of interest.

REFERENCES

1. Giedyk M, Goliszewska K, Gryko D. Vitamin B12catalysed reactions. Chemical Society Reviews. 2015;44(11):3391-404.
2. Acevedo-Rocha CG, Gronenberg LS, Mack M, Commichau FM, Genee HJ. Microbial cell factories for the sustainable manufacturing of B vitamins. Current Opinion in

Biotechnology. 2019;56:18-29.
3. Kräutler B. Vitamin B12: chemistry and biochemistry. Biochemical Society Transactions. 2005;33(4):806-10.
4. Banerjee R, Ragsdale SW. The Many Faces of Vitamin B12: Catalysis by Cobalamin-Dependent Enzymes. Annual Review of Biochemistry. 2003;72(1):209-47.
5. Chamlagain B, Deptula P, Edelmann M, Kariluoto S, Grattepanche F, Lacroix C, et al. Effect of the lower ligand precursors on vitamin B12 production by food-grade Propionibacteria. LWT - Food Science and Technology. 2016;72:117-24.
6. Anderson PJ, Lango J, Carkeet C, Britten A, Kräutler B, Hammock BD, et al. One Pathway Can Incorporate either Adenine or Dimethylbenzimidazole as an α-Axial Ligand of B12 Cofactors in Salmonella enterica. Journal of Bacteriology. 2007;190(4):1160-71.
7. Torres AC, Vannini V, Bonacina J, Font G, Saavedra L, Taranto MP. Cobalamin production by Lactobacillus coryniformis: biochemical identification of the synthetized corrinoid and genomic analysis of the biosynthetic cluster. BMC Microbiology. 2016;16(1).
8. Piwowarek K, Lipińska E, Hać-Szymańczuk E, Kieliszek M, Ścibisz I. Propionibacterium spp.—source of propionic acid, vitamin B12, and other metabolites important for the industry. Applied Microbiology and Biotechnology. 2017;102(2):515-38.
9. Fang H, Kang J, Zhang D. Microbial production of vitamin B12: a review and future perspectives. Microbial Cell Factories. 2017;16(1).
10. Martens HBMWDJJH. Microbial production of vitamin B 12. Applied Microbiology and Biotechnology. 2002;58(3):275-85.
11. Ojala T, Laine PKS, Ahlroos T, Tanskanen J, Pitkänen S, Salusjärvi T, et al. Functional genomics provides insights into the role of Propionibacterium freudenreichii ssp. shermanii JS in cheese ripening. International Journal of Food Microbiology. 2017;241:39-48.
12. Chamlagain B, Sugito TA, Deptula P, Edelmann M, Kariluoto S, Varmanen P, et al. In situproduction of active vitamin B12 in cereal matrices usingPropionibacterium freudenreichii. Food Science & Nutrition. 2017;6(1):67-76.
13. Navone L, McCubbin T, Gonzalez-Garcia RA, Nielsen LK, Marcellin E. Genome-scale model guided design of Propionibacterium for enhanced propionic acid production. Metabolic Engineering Communications. 2018;6:1-12.
14. Liu L, Zhu Y, Li J, Wang M, Lee P, Du G, et al. Microbial production of propionic acid from propionibacteria: Current state, challenges and perspectives. Critical Reviews in Biotechnology. 2012;32(4):374-81.
15. Thierry A, Deutsch S-M, Falentin H, Dalmasso M, Cousin FJ, Jan G. New insights into physiology and metabolism of Propionibacterium freudenreichii. International Journal of Food Microbiology. 2011;149(1):19-27.
16. Angelopoulou A, Alexandraki V, Georgalaki M, Anastasiou R, Manolopoulou E, Tsakalidou E, et al. Production of probiotic Feta cheese using Propionibacterium freudenreichii subsp. shermanii as adjunct. International Dairy Journal. 2017;66:135-9.
17. Moore SJ, Lawrence AD, Biedendieck R, Deery E, Frank S, Howard MJ, et al. Elucidation of the anaerobic pathway for the corrin component of cobalamin (vitamin B12). Proceedings of the National Academy of Sciences. 2013;110(37):14906-11.
18. Iida K, Kajiwara M. Metabolic pathways leading from amino acids to vitamin B12 in Propionibacterium shermanii, and the sources of the seven methyl carbons: Metabolic pathways from amino acids to vitamin B12. *FEBS Journal*. 2007;274(19):5090-5095. doi:10.1111/j.1742-4658.2007.06028.x
19. Deptula P, Kylli P, Chamlagain B, Holm L, Kostiainen R, Piironen V, et al. BluB/CobT2 fusion enzyme activity reveals mechanisms responsible for production of active form of vitamin B12 by Propionibacterium freudenreichii. Microbial Cell Factories. 2015;14(1).
20. Taga ME, Larsen NA, Howard-Jones AR, Walsh CT, Walker GC. BluB cannibalizes flavin to form the lower ligand of vitamin B12. Nature. 2007;446(7134):449-53.
21. Hazra Amrita B, Tran Jennifer LA, Crofts Terence S, Taga Michiko E. Analysis of Substrate Specificity in CobT Homologs Reveals Widespread Preference for DMB, the Lower Axial Ligand of Vitamin B12. Chemistry & Biology. 2013;20(10):1275-85.
22. Crofts Terence S, Seth Erica C, Hazra Amrita B, Taga Michiko E. Cobamide Structure Depends on Both Lower Ligand Availability and CobT Substrate Specificity. Chemistry & Biology. 2013;20(10):1265-74.
23. Roessner CA, Scott AI. Fine-Tuning Our Knowledge of the Anaerobic Route to Cobalamin (Vitamin B12). Journal of Bacteriology. 2006;188(21):7331-4.
24. Frank S, Brindley AA, Deery E, Heathcote P, Lawrence AD, Leech HK, et al. Anaerobic synthesis of vitamin B12: characterization of the early steps in the pathway. Biochemical Society Transactions. 2005;33(4):811-4.
25. Johnson OA, Affam AC. Petroleum sludge treatment and disposal: A review. Environmental Engineering Research. 2018;24(2):191-201.
26. Hu G, Li J, Zeng G. Recent development in the treatment of oily sludge from petroleum industry: A review. Journal of Hazardous Materials. 2013;261:470-90.
27. da Silva LJ, Alves FC, de França FP. A review of the technological solutions for the treatment of oily sludges from petroleum refineries. Waste Management & Research. 2012;30(10):1016-30.
28. Varjani S, Upasani VN, Pandey A. Bioremediation of oily sludge polluted soil employing a novel strain of Pseudomonas aeruginosa and phytotoxicity of petroleum hydrocarbons for seed germination. Science of The Total Environment. 2020;737:139766.
29. Jasmine J, Mukherji S. Impact of bioremediation strategies on slurry phase treatment of aged oily sludge from a refinery. Journal of Environmental Management. 2019;246:625-35.
30. Cerqueira VS, Hollenbach EB, Maboni F, Vainstein MH, Camargo FAO, Peralba MdCR, et al. Biodegradation potential of oily sludge by pure and mixed bacterial cultures. Bioresource Technology. 2011;102(23):11003-10.
31. Liu YJ, Chen YP, Jin PK, Wang XC. Bacterial communities in a crude oil gathering and transferring system (China). Anaerobe. 2009;15(5):214-8.
32. Shahavi MH, Hosseini M, Jahanshahi M, Meyer RL, Darzi

GN. Evaluation of critical parameters for preparation of stable clove oil nanoemulsion. Arabian Journal of Chemistry. 2019;12(8):3225-30.
33. Mofidian R, Barati A, Jahanshahi M, Shahavi MH. Optimization on thermal treatment synthesis of lactoferrin nanoparticles via Taguchi design method. SN Applied Sciences. 2019;1(11).
34. Hedayatnasab Z, Abnisa F, Daud WMAW. Review on magnetic nanoparticles for magnetic nanofluid hyperthermia application. Materials & Design. 2017;123:174-96.
35. Tartaj P, Morales MP, González-Carreño T, Veintemillas-Verdaguer S, Serna CJ. Advances in magnetic nanoparticles for biotechnology applications. Journal of Magnetism and Magnetic Materials. 2005;290-291:28-34.
36. Olle B, Bucak S, Holmes TC, Bromberg L, Hatton TA, Wang DIC. Enhancement of Oxygen Mass Transfer Using Functionalized Magnetic Nanoparticles. Industrial & Engineering Chemistry Research. 2006;45(12):4355-63.
37. Labbeiki G, Attar H, Heydarinasab A, Sorkhabadi S, Rashidi A. Enhanced oxygen transfer rate and bioprocess yield by using magnetite nanoparticles in fermentation media of erythromycin. DARU Journal of Pharmaceutical Sciences. 2014;22(1).
38. Jiang J-Z, Zhang S, Fu X-L, Liu L, Sun B-M. Review of gas–liquid mass transfer enhancement by nanoparticles from macro to microscopic. Heat and Mass Transfer. 2019;55(8):2061-72.
39. Rahmanzadeh L, Ghorbani M, Jahanshahi M. Synthesis and Characterization of Fe3O4@ Polyrhodanine Nanocomposite with Core-Shell Morphology. Advances in Polymer Technology. 2014;33(S1):n/a-n/a.
40. Gunanto YE, Izaak MP, Jobiliong E, Cahyadi L, Adi WA. High purity Fe3O4 from Local Iron Sand Extraction. Journal of Physics: Conference Series. 2018;1011:012005.
41. Simamora P, Saragih CS, Hasibuan DP, Rajagukguk J. Synthesis of nanoparticles Fe 3 O 4 /PEG/PPy-based on natural iron sand. Materials Today: Proceedings. 2018;5(7):14970-4.
42. Van Wyk J, Britz TJ. A rapid HPLC method for the extraction and quantification of vitamin B12in dairy products and cultures ofPropionibacterium freudenreichii. Dairy Science & Technology. 2010;90(5):509-20.
43. Karade VC, Dongale TD, Sahoo SC, Kollu P, Chougale AD, Patil PS, et al. Effect of reaction time on structural and magnetic properties of green-synthesized magnetic nanoparticles. Journal of Physics and Chemistry of Solids. 2018;120:161-6.
44. Hernández-Hernández AA, Álvarez-Romero GA, Castañeda-Ovando A, Mendoza-Tolentino Y, Contreras-López E, Galán-Vidal CA, et al. Optimization of microwave-solvothermal synthesis of Fe3O4 nanoparticles. Coating, modification, and characterization. Materials Chemistry and Physics. 2018;205:113-9.
45. Cushing BL, Kolesnichenko VL, O'Connor CJ. Recent Advances in the Liquid-Phase Syntheses of Inorganic Nanoparticles. Chemical Reviews. 2004;104(9):3893-946.
46. Rahmawati R, Permana MG, Harison B, Nugraha, Yuliarto B, Suyatman, et al. Optimization of Frequency and Stirring Rate for Synthesis of Magnetite (Fe 3 O 4) Nanoparticles by Using Coprecipitation- Ultrasonic Irradiation Methods. Procedia Engineering. 2017;170:55-9.
47. Hajfarajollah H, Mokhtarani B, Mortaheb H, Afaghi A. Vitamin B12 biosynthesis over waste frying sunflower oil as a cost effective and renewable substrate. Journal of Food Science and Technology. 2014.
48. Nasreen Z, Kalsoom S. Biodegradation of petroleum industry oily sludge and its application in land farming: a review. International Journal of Environment and Waste Management. 2018;21(1):37.
49. Yan P, Lu M, Yang Q, Zhang H-L, Zhang Z-Z, Chen R. Oil recovery from refinery oily sludge using a rhamnolipid biosurfactant-producing Pseudomonas. Bioresource Technology. 2012;116:24-8.
50. Hajfarajollah H, Mokhtarani B, Noghabi KA. Newly Antibacterial and Antiadhesive Lipopeptide Biosurfactant Secreted by a Probiotic Strain, Propionibacterium Freudenreichii. Applied Biochemistry and Biotechnology. 2014;174(8):2725-40.
51. Pritchard GG, Wimpenny JWT, Morris HA, Lewis MWA, Hughes DE. Effects of Oxygen on Propionibacterium shermanii Grown in Continuous Culture. Journal of General Microbiology. 1977;102(2):223-33.
52. Quesada-Chanto A, Schmid-Meyer AC, Schroeder AG, Carvalho-Jonas MF, Blanco I, Jonas R. Effect of oxygen supply on biomass, organic acids and vitamin B12 production by Propionibacterium shermanii. *World Journal of Microbiology and Biotechnology*. 1998;14(6):843-846. doi:10.1023/A:1008868907251
53. Galaction A-I, Cascaval D, Turnea M, Folescu E. Enhancement of oxygen mass transfer in stirred bioreactors using oxygen-vectors 2. Propionibacterium shermanii broths. Bioprocess and Biosystems Engineering. 2005;27(4):263-71.
54. Wang P, Zhang Z, Jiao Y, Liu S, Wang Y. Improved propionic acid and 5,6-dimethylbenzimidazole control strategy for vitamin B12 fermentation by Propionibacterium freudenreichii. Journal of Biotechnology. 2015;193:123-9.